

Article

# Adaptive PMSM Control of Ship Electric Propulsion with Energy-Saving Features

Zenon Zwierzewicz, Dariusz Tarnapowicz \*  and Arkadiusz Nerć

Faculty of Mechatronics and Electrical Engineering, Maritime University of Szczecin, Willowa 2, 71-650 Szczecin, Poland; z.zwierzewicz@pm.szczecin.pl (Z.Z.); a.nerc@pm.szczecin.pl (A.N.)

\* Correspondence: d.tarnapowicz@pm.szczecin.pl; Tel.: +48-9148-09-955

**Abstract:** Electric ship propulsion is considered one of the most promising alternatives to conventional combustion systems. Its goal is to reduce the carbon footprint and increase a ship's maneuverability, operational safety, and reliability. The high requirements for ship propulsion make permanent magnet synchronous motors (PMSMs) an attractive solution due to their characteristics. This paper discusses the control problem of a PMSM based on the input–output feedback linearization method combined with the optimal and adaptive control techniques. The method presented here integrates the parameter tuning process with the optimal design of the baseline controller. Since the load disturbances are treated as an additional unknown parameter, there is no need to introduce an integral action to deal with the resulting steady-state error. An important feature of the designed controller is the so-called energetic optimization of the system; i.e., in addition to the aforementioned adaptive and optimal controller, it has a feature of ensuring zero reactive power consumed by the system. The performed simulations of the machine speed stabilization process confirmed the high efficiency of the proposed controller despite the assumed uncertainty of the system parameters and environmental (load) disturbances. Besides achieving high-quality control, an essential feature of this approach is the elimination of the tuning problem.

**Keywords:** PMSM; control system design; adaptive control; optimal control; energy efficiency



**Citation:** Zwierzewicz, Z.; Tarnapowicz, D.; Nerć, A. Adaptive PMSM Control of Ship Electric Propulsion with Energy-Saving Features. *Energies* **2024**, *17*, 2178. <https://doi.org/10.3390/en17092178>

Academic Editor: José Matas

Received: 22 March 2024

Revised: 21 April 2024

Accepted: 30 April 2024

Published: 2 May 2024



**Copyright:** © 2024 by the authors. Licensee MDPI, Basel, Switzerland. This article is an open access article distributed under the terms and conditions of the Creative Commons Attribution (CC BY) license (<https://creativecommons.org/licenses/by/4.0/>).

## 1. Introduction

In recent years, electric ship propulsion has become an important alternative to the commonly used combustion drives. This applies to both small all-electric ships (with their own energy storage) and large seagoing ships in the diesel–electric solution [1]. This is related to the very high requirements placed on engineers designing ship drives in terms of reducing the carbon footprint and other environmental problems (e.g., noise, vibrations). The International Maritime Organization has defined stringent requirements for improving ship energy efficiency by introducing the Energy Efficiency Design Index (EEDI) [2]. Figure 1 shows opportunities for improving EEDI [3].

As improving the energy efficiency of a vessel through technological change is a major challenge for engineers due to technological limitations, improvement through speed optimization (reduction) is now common practice. This situation stimulates the continuous technological development of all components affecting the energy efficiency of a ship. Increasing energy efficiency by reducing losses (a solution proposed in this article) will improve EEDI (which is implied in the definition of EEDI) while improving the economic effect.

PMSM, compared to the commonly used Electrically Excited Synchronous Motors and, less frequently, Squirrel Cage Motors used in ship drives, in addition to the well-known advantages (such as higher power density, high reliability, lower vibrations, lower weight and dimensions) are characterized by higher efficiency (especially when the motor is underloaded), mainly due to the elimination of excitation losses (from 3 to 6%, depending

on the load and motor power) [4–7]. Due to the possibility of using a large number of pole pairs, the use of gears is not required (gear losses are approximately 2%, depending on the number of gear stages), which also increases the efficiency [8,9].

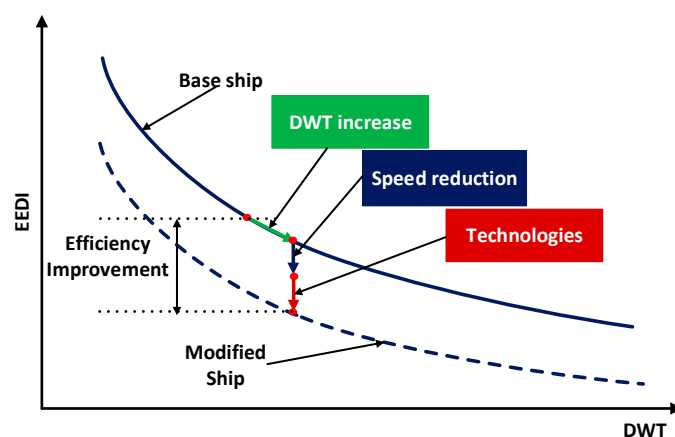


Figure 1. Opportunities to improve the EEDI coefficient [3].

An additional benefit of using a ship’s electric drive is its maneuverability (flexibility and dynamics), which is particularly useful on passenger, port and inland ships.

The requirements for the ship’s propulsion are high due to the specific nature of the drive’s operation. There are frequent and sudden changes in load while maintaining a constant propeller speed (especially in rough seas—immersion and emergence of the propeller).

The main task of the PMSM control system is to ensure appropriate drive dynamics. Regardless of the control strategy, the control method consists of decoupling the state variables: PMSM electromagnetic flux and torque [10]. Two basic categories of control can be distinguished: control based on the general algorithm of vector control of AC drives, consisting in the orientation of the stator current vector relative to the rotor flux (Field Oriented Control—FOC) and direct control of the electromagnetic torque and flux (Direct Torque Control—DTC) [10–13].

FOC control has become the most popular in recent years due to the low requirements for the control system. Among the various strategies and control systems according to the FOC method, the most frequently implemented is control maintaining a constant power angle (angle between the stator current vector and the rotor flux) [10]. This is performed in a synchronously rotating  $d, q$  coordinate system so that the  $d$  axis coincides with the axis of the rotating magnet, and the  $q$  axis is perpendicular to it. The stator current has only one component in the  $q$  axis ( $I_s = I_q$ ) and is directly responsible for the torque. The control system with linear Proportional and Integral (PI) controllers allows the speed (or torque) of the PMSM to be controlled [12–15]. PI controllers are commonly used in PMSM drives (using the FOC control method). They are considered one of the simplest control techniques and offer adequate performance. However, PI controllers are not the best choice for applications where high efficiency and precision are required [14].

In [15], a modification of the classical FOC method with energy optimization was proposed, allowing for the reduction in reactive power in the INV-PMSG circuit to zero. Despite the effectiveness of control with additional energy optimization ( $Q = 0$ ), testing using the FOC method, which involves analyzing the circuit in a steady state, has shown its drawbacks, i.e., oscillations of the electromagnetic moment with dynamic changes in load or speed. This is caused, in accordance with the idea of the classical FOC method, by the lack of control during the transition period. The reduction in reactive power in propulsion systems with PMSMs is widely described in the literature, but it mainly concerns the converter supply circuit (AC/DC), not the INV-PMSM circuit analyzed in [15–17].

The problem of adaptive and/or optimal control of PMSM machine has been addressed in many papers with the use different approaches and algorithms. To mention

a few, in [18], the authors designed a classical cascade control structure with the inner (current) loop built using an optimal linear–quadratic regulator (LQR)-type controller, while the speed controller, in the outer control loop, is of the PI adaptive type. However, to determine the optimal controller gains, one needs the system parameters to be known and, on the other hand, the overall system optimal performance cannot be achieved here.

Many works in this context start from the position of the adaptive dynamic programming method; e.g., in [19], to avoid using the conventional cascade PI structure, the authors transformed the PSM model via feedforward control inputs, obtaining the speed and current tracking problem with augmented control  $u = [i_d \ i_q \ u_d \ u_q]$ , also taking into account the saturation of voltages. The obtained new control problem was then treated as a non-linear optimal control task. To solve this new formulated problem adaptive dynamic programming method was used. The optimal solution of the ensuing Hamilton–Jacobi–Issac equation, which provides the value to the control law, was approximated by a simple online approximator. However, such modern and advanced approaches appear to be too complex and demanding for standard practical applications (implementations).

A classical PI controller coupled with an adaptive speed observer was analyzed in [20]. Although a speed sensor is not required here, the problem of PI controller tuning still remains.

In this article, the authors presented a properly designed control with features such as self-adjusting regulator settings for various operating conditions, optimal control in the transient state and reduction in reactive power to zero. Therefore, proper control aims to ensure not only the high efficiency of the engine, but also to make it a self-operated device. Reducing reactive power to zero in the INV-PMSM circuit facilitates a reduction in losses in the inverter, power cables and the machine by approximately 10% [21].

The main objective of the paper is to propose a PMSM speed controller design based on its nonlinear mathematical model. It is assumed that the model parameters are unknown, as are the external disturbances. In order to meet the requirements listed above, the synthesis of the controller is based on optimal and adaptive control techniques, in particular, on an adaptive version of the standard output feedback linearization method [22,23]. Model basis function approximators [24] are proposed to cope with unknown plant parameters. During the routine work of the PMSM (i.e., under specified steady-state conditions), besides modeling errors, the load disturbances  $d$  also have to be taken into account. These disturbances lead to the steady speed error which can be typically compensated by the integral action introduced to the control system. To avoid the problems, inherent in the use of the integral action, the load disturbances and other constant modeling errors are treated as an unknown additional parameter to be addressed adaptively.

The novelty of the paper is the approach using adaptive output feedback linearization combined with LQR optimization, the analysis of system inner (zero) dynamics and the guarantee of system reactive power zeroing. In none of the known publications do the above-mentioned elements appear together and in such a form.

Improving the efficiency of the PMSM drive by reducing reactive power during energy conversion has been widely described in the literature, focusing primarily on the converter power supply circuit [16,25,26]. There are few publications on limiting the start-up in the converter machine circuit (INV-PMSM), and the proposed methods for improving the energy efficiency of the system are complicated and ineffective [27,28]. The authors proposed a solution to reduce reactive power in the converter machine circuit (INV-PMSM), which facilitates a reduction in losses in the INV, transmission line and PMSM.

In this paper, it has been proven that the introduced parameter tuning method guarantees the asymptotic stability of the system. One may say that, besides general system model structure (which is well known), no extra knowledge is here required.

The paper is divided into five sections and ends with conclusions. The principal concept of PMSM models and the adaptive control techniques are given in Section II. The designing of an optimal and adaptive speed stabilization controller is presented in Section III. In Section IV, the overall results of the work are discussed. Finally, Section V includes the final discussion and conclusions.

## 2. Models and Methods

### 2.1. General Model Structure and the Statement of Control Problem

The mathematical description of PMSM is performed in the synchronously rotating system of  $d, q$  coordinates, which are closely related to its magnetic field. The  $d$  axis coincides with the magnetic field vector, while the electromagnetic force  $E$  will then coincide with the  $q$  axis. The nonlinear model of the PMSM machine in the rotor reference frame ( $d, q$  frame) can be written in the form of the following system of differential equations:

$$\begin{aligned} U_d(t) &= r_1 I_d(t) + L_1 \frac{dI_d(t)}{dt} - \omega L_1 I_q(t), \\ U_q(t) &= r_1 I_q(t) + L_1 \frac{dI_q(t)}{dt} + \omega L_1 I_d(t) + \psi_0 \omega. \end{aligned} \quad (1)$$

where the following are defined:

$U_d(t), U_q(t), I_d(t), I_q(t)$ —the inverter output voltage and stator currents (PMSM) on  $d, q$  axes.

$\psi_0$ —the modulus of the flux vector  $\bar{\Psi}_0$  of PMSM excitation;

$\omega$ —the angular speed of sinusoidal state variables in the machine (this is so-called electric speed);

$r_1, L_1$ —resistance and inductance of phase stator windings.

$$T_e = 1.5p\psi_0 I_q(t) \quad (2)$$

where the following are defined:

$p$ —the number of pairs of magnetic poles;

$\omega_m = \frac{\omega}{p}$ —the angular speed of PMSM rotor rotation (this is so-called mechanical speed);

$T_e$ —PMSM electromagnetic torque.

$$J \frac{d\omega_m}{dt} = T_e - T_L \quad (3)$$

where the following are defined:

$T_L$ —load torque;

$J$ —moment of inertia.

By analyzing the system (1), (2), (3), it is easy to notice that for specified  $\omega_m$  and  $T_L$ , there are an infinite number of equilibrium points (steady states) of the system, associated with input pairs  $(U_d, U_q)$ .

Therefore, there is a natural problem of selecting a pair of inputs (controls)  $U_d^*, U_q^*$  in such a way to ensure the reset of the system's reactive power ( $Q = 0$ ), which we will refer to as energy optimization.

The control problem is twofold:

1. Design a feedback control system generating pairs of inputs (controls)  $(U_d, U_q)$  to stabilize the angular velocity of the machine rotor  $\omega_m$ , despite load disturbances  $T_L$ , assuming that the system parameters are unknown and the transient dynamics is optimized;
2. Using the fact of an infinite number of steady-state solutions from point 1, find the  $U_d^*, U_q^*$  controllers ensuring that the system's reactive power is zeroed ( $Q = 0$ ).

### 2.2. Theoretical Introduction to the Adaptive Control Methods Used

To cope with the problem formulated above, the main concept of the adaptive control technique applied here and its formal proof in the form of a detailed analysis of the system output stabilization problem are now presented. For simplicity and clarity, but without loss of generality, the following second-order nonlinear affine system, SISO, is considered of the form:

$$\begin{aligned} \dot{x}_1 &= x_2 \\ \dot{x}_2 &= f(x_1, x_2) + cu + d(t) \\ y &= x_1 \end{aligned} \quad (4)$$

where the following are defined:

$x_1, x_2$ —state variables;

$u$ —control variable;

$y$ —system output;

$f$  and  $c$ —known function and constant, respectively;

$d$ —known disturbance.

However, it should be noted that these considerations also apply to a general nonlinear system in Brunovsky canonical form [29]. For the time being, it is also assumed that the system is completely known.

It is easy to see that to stabilize the system output at the assumed setpoint  $x_{1d}$  it is enough to apply a simple feedback linearizing controller of the form:

$$u = \frac{-f(x_1, x_2) - d + v}{c} \quad (5)$$

where  $x_{1d}$  is the desired output and  $v$  some sub controller,

Denoting  $e_1 = x_{1d} - x_1, e_2 = x_2$ , the obtained system takes the form:

$$\begin{cases} \dot{e}_1 = e_2 \\ \dot{e}_2 = v \end{cases} \quad (6)$$

Now, taking  $v = k_1 e_1 + k_2 e_2$ , we can see that the controller gains  $k_1$  and  $k_2$  can be easily determined by one of the standard methods, e.g., pole placement or LQR techniques [30].

To be more realistic, we now assume that the function  $f$  and the disturbance  $d$  are unknown but can be represented as a linear combination of some known basis functions:

$$F = \underbrace{\theta_1 \varphi_1 + \dots + \theta_n \varphi_n}_f + \underbrace{\theta_{n+1}}_d \quad (7)$$

where  $\varphi_i$  are known basis functions,  $\theta_i$  are constant but unknown system parameters and  $\theta_{n+1} = d$ , i.e., the disturbance is treated as an unknown constant parameter.

Let  $\hat{\theta}_i$  denote the estimates of the parameters  $\theta_i$  and let:

$$\tilde{\theta}_i = \theta_i - \hat{\theta}_i \quad (8)$$

Hence,

$$\hat{F} = \hat{\theta}_1 \varphi_1 + \dots + \hat{\theta}_n \varphi_n + \hat{\theta}_{n+1} \text{ and } \hat{\theta}_{n+1} = \hat{d} \quad (9)$$

Now, taking control  $u$  as:

$$u = \frac{-\hat{F} + v}{c} = \frac{-(\hat{\theta}_1 \varphi_1 + \dots + \hat{\theta}_n \varphi_n + \hat{\theta}_{n+1}) + v}{c} \quad (10)$$

where  $v$  stands for a subsidiary control, yields

$$\begin{cases} \dot{e}_1 = e_2 \\ \dot{e}_2 = v + \underbrace{(\tilde{\theta}_1 \varphi_1 + \dots + \tilde{\theta}_n \varphi_n + \tilde{\theta}_{n+1})}_{\varepsilon} \end{cases} \quad (11)$$

Note that since the term  $\varepsilon$  in parentheses is unknown, the system is not necessarily stable.

One idea to solve this stability problem seems to be an appropriate tuning of the parameter estimates  $\hat{\theta}_i$  to ensure system stabilization.

In the following, using the Lyapunov approach, a formula is derived for tuning the parameters  $\hat{\theta}_i$  in such a way as to ensure asymptotic stability for the system (11).

To this end, write (11) in the matrix form

$$\begin{bmatrix} \dot{e}_1 \\ \dot{e}_2 \end{bmatrix} = \underbrace{\begin{bmatrix} 0 & 1 \\ 0 & 0 \end{bmatrix}}_A \begin{bmatrix} e_1 \\ e_2 \end{bmatrix} + \underbrace{\begin{bmatrix} 0 \\ 1 \end{bmatrix}}_B v + \underbrace{\begin{bmatrix} 0 \\ 1 \end{bmatrix}}_B (\tilde{\theta}_1 \varphi_1 + \dots + \tilde{\theta}_n \varphi_n + \tilde{\theta}_{n+1}) \quad (12)$$

and denote

$$\chi = [e_1, e_2]^T \quad (13)$$

$$\dot{\chi} = A\chi + Bv + B\Phi^T \tilde{\theta} \quad (14)$$

$$\tilde{\theta} = [\tilde{\theta}_1, \dots, \tilde{\theta}_n, \tilde{\theta}_{n+1}]^T, \Phi = [\varphi_1, \dots, \varphi_n, 1]^T, \Gamma = \text{diag}[\gamma_1, \dots, \gamma_n, \gamma_{n+1}] \quad (15)$$

where  $\Gamma$  is a diagonal matrix of tuning parameters.

Let the Lyapunov function now be chosen (more precisely, a candidate for the Lyapunov function) in the form:

$$V = \chi^T P \chi + \tilde{\theta}^T \Gamma^{-1} \tilde{\theta} \quad (16)$$

where  $P = [p_{ij}] > 0$ , i.e., a positively defined matrix.

The time derivative of  $V$ , along with the solutions of the tracking error dynamics equation, is:

$$\begin{aligned} \dot{V} &= \dot{\chi}^T P \chi + \chi^T P \dot{\chi} + 2\tilde{\theta}^T \Gamma^{-1} \dot{\tilde{\theta}} = (\chi^T A^T + v^T B^T + \tilde{\theta}^T \Phi B^T +) P \chi + \\ &\quad + \tilde{\theta}^T \Phi B^T P \chi + \chi^T P (A\chi + Bv + B\Phi^T \tilde{\theta}) + 2\tilde{\theta}^T \Gamma^{-1} \dot{\tilde{\theta}} = \\ &= \chi^T (A^T P + PA) \chi + 2\chi^T P B v + 2\tilde{\theta}^T \Phi B^T P \chi + 2\tilde{\theta}^T \Gamma^{-1} \dot{\tilde{\theta}} = \end{aligned} \quad (17)$$

Assuming control  $v$  as

$$v = \frac{1}{r} B^T P \chi = k^T \chi \quad (18)$$

yields

$$\begin{aligned} &= \underbrace{\chi^T (A^T P + PA - \frac{2}{r} P B B^T P)}_* \chi + 2\tilde{\theta}^T \underbrace{(\Phi B^T P \chi + \Gamma^{-1} \dot{\tilde{\theta}})}_{=0} = -(\chi^T Q \chi + r v^2) \\ &\leq 0 \end{aligned} \quad (19)$$

Taking into account that  $v^2 = \frac{1}{r^2} \chi^T P B B^T P \chi$ , denoting the term  $*$   $\triangleq -(\chi^T Q \chi + r v^2)$  (where  $Q > 0$  and  $r > 0$ ) as well as making the term in the second bracket equal to zero (see (21)), one can obtain  $\dot{V} \leq 0$ , thereby establishing that  $\chi$  and  $\theta$  are bounded. However, according to Barbalat's Lemma [22], it can be inferred that  $\lim_{t \rightarrow \infty} \chi(t) = 0$ , cf. [24], obtaining the system asymptotic stability. To address the parameter drift problem via the  $\sigma$ -modification method, see [31].

What is more, it can be seen that the matrix  $P$  is a solution of the algebraic Riccati equation:

$$A^T P + PA - \frac{1}{r} P B B^T P + Q = 0 \quad (20)$$

coupled to the standard linear quadratic problem, where  $\dot{\chi} = A\chi + Bv$  is a linear system dynamics and  $J(v) = \int_0^\infty (\chi^T Q \chi + r v^2) dt$  is optimization criterion.

Consequently, an optimal (sub)controller and the parameter adaptation law has been obtained in the form:

$$v = \frac{1}{r} B^T P \chi = k^T \chi = r^{-1} [p_{21}, p_{22}] \begin{bmatrix} e_1 \\ e_2 \end{bmatrix} = r^{-1} (p_{21} e_1 + p_{22} e_2) = k_1 e_1 + k_2 e_2 \quad (21)$$

$$\dot{\tilde{\theta}} = -\Gamma \Phi B^T P \chi \xrightarrow{\text{see(5)}} \dot{\hat{\theta}} = \Gamma \Phi B^T P \chi \Rightarrow \hat{\theta}(t) = \Gamma \int_0^t \Phi B^T P \chi d\tau \quad (22)$$

Or in expanded form:

$$\begin{aligned} \hat{\theta}_1(t) &= \gamma_1 \int_0^t \varphi_1(p_{21}e_1 + p_{22}e_2)d\tau \\ &\vdots \\ \hat{\theta}_n(t) &= \gamma_n \int_0^t \varphi_n(p_{21}e_1 + p_{22}e_2)d\tau \\ \hat{\theta}_{n+1}(t) &= \gamma_{n+1} \int_0^t (p_{21}e_1 + p_{22}e_2)d\tau \end{aligned} \quad (23)$$

Concluding, the solution to the optimal, adaptive control (stabilization) problem formulated above, represented by the dynamics (4), unknown nonlinearity  $f$  and unknown load disturbance  $d$ , is given by Formulas (21), (23) and (10), where  $c$  is taken as a design parameter.

### 3. Designing an Optimal and Adaptive PMSM Speed Stabilization Controller

Using the theoretical results of Section 2.2, an optimal and adaptive controller for PMSM speed stabilization also including system energetic optimization will now be designed.

#### 3.1. Conversion of the Machine Model to the Appropriate Form via I/O Linearization Method—Nonadaptive Version of Controller Synthesis

To facilitate the analysis and for the sake of clarity, the traditional notations in the control theory have been adopted. Let, at first, the model (1), (2), (3) be written in the following state-space form:

$$\begin{aligned} \dot{x}_1 &= -\frac{r_1}{L_1}x_1 + px_3x_2 + \frac{1}{L_1}u_1 \\ \dot{x}_2 &= -px_3x_1 - \frac{r_1}{L_1}x_2 - \frac{p\psi_0}{L_1}x_3 + \frac{1}{L_1}u_2 \\ \dot{x}_3 &= \frac{1.5p\psi_0}{J}x_2 - \frac{1}{J}T_L \end{aligned} \quad (24)$$

where the following are defined:

$$[x_1, x_2, x_3]^T = [I_d, I_q, \omega_m]^T \text{—system state;}$$

$$[u_1, u_2]^T = [U_d, U_q]^T \text{—control vector.}$$

The considered control problem is to stabilize the state variable  $x_3$  on the desired  $x_3^*$  value; i.e., bring the system output:

$$y = x_3 - x_3^* \quad (25)$$

to zero, by using control variables  $u_1$  and  $u_2$ , where  $x_3^* = \omega_m^*$  denotes the desired value of  $\omega_m$ .

Analyzing the form of the above nonlinear system (24), one can observe that for controlling the output  $y$ , it is enough to manipulate only the control variable  $u_2$ , while  $u_1$  may serve us as an extra control parameter which will be then used for the system energetic optimization.

The synthesis of control  $u_2$  can be performed by the input–output (I/O) feedback linearization, a method well known in the field of nonlinear control system engineering [22].

Based on this method, the model of (24) and (25) is transformed to the canonical form suitable for direct derivation of the control law  $u_2$ .

However, to avoid the Lie derivative formalism, specifically here, the output of (25) is repeatedly differentiated with respect to time until control  $u_2$  appears.

First, we denote  $y_1 = y$

Hence, using (24), we obtain:

$$\dot{y}_1 = \frac{1.5p\psi_0}{J}x_2 - \frac{T_L}{J} \triangleq y_2 \quad (26)$$

Differentiating (26) once more (and again using (24)), we have:

$$\dot{y}_2 = \frac{1.5p\psi_0}{JL_1}(-pL_1x_3x_1 - r_1x_2 - p\psi_0x_3 + u_2) \quad (27)$$

Thus, the canonical form of some (sub)system of (24) was obtained (cf. (4)):

$$\begin{aligned} \dot{y}_1 &= y_2 \\ \dot{y}_2 &= f(\mathbf{x}) + g(\mathbf{x})u_2 \end{aligned} \quad (28)$$

where

$$\begin{aligned} y_1 &= \mathbf{y} = x_3 - x_3^* \\ y_2 &= \dot{y}_1 = \frac{1.5p\psi_0}{J}x_2 - \frac{T_f}{J}. \end{aligned} \quad (29)$$

and

$$\begin{aligned} f(\mathbf{x}) &= \frac{1.5p\psi_0}{JL_1}(-pL_1x_3x_1 - r_1x_2 - p\psi_0x_3), \\ g(\mathbf{x}) &= c = \frac{1.5p\psi_0}{JL_1}. \end{aligned} \quad (30)$$

So, the nonadaptive controller version is [4]:

$$u_2 = \frac{-f(\mathbf{x}) + v}{c} = \frac{-\frac{1.5p\psi_0}{JL_1}(-pL_1x_3x_1 - r_1x_2 - p\psi_0x_3) - v}{\frac{1.5p\psi_0}{JL_1}} = (r_1x_2 + p\psi_0x_3 + pL_1x_3x_1) - \frac{JL_1}{1.5p\psi_0}v \quad (31)$$

where

$$v = k_1y_1 + k_2y_2 = k_1y + k_2\dot{y} \quad (32)$$

Now assuming that the system parameters are known, the gains  $k_1$  and  $k_2$  of this PD-type controller can be easily obtained by the pole placement method or the LQR algorithm [4].

### 3.2. Optimal and Adaptive Controller Synthesis—Basic Case

Since the system (28) is of the form (4), the theory presented in Section 2.2. can further be applied. Therefore, the previous assumption requiring knowledge of the system parameters can now be rejected.

To this end, let us write (31) in the standard parametric form

$$u_2 = (\hat{\theta}_1x_2 + \hat{\theta}_2x_3 + \hat{\theta}_3x_3x_1) - \hat{c}v \quad (33)$$

where  $\hat{c} = \frac{1}{c}$  is a design parameter.

Now, assuming that

$$\hat{\theta} = [\hat{\theta}_1, \hat{\theta}_2, \hat{\theta}_3]^T, \quad \Phi = [\varphi_1, \varphi_2, \varphi_3]^T = [x_2, x_3, x_3x_1]^T \quad (34)$$

the final formula for control  $u_2$  is obtained (cf. (21)):

$$\begin{aligned} u_2 &= \hat{\theta}^T \Phi + \hat{c}k^T \chi = (\hat{\theta}_1x_2 + \hat{\theta}_2x_3 + \hat{\theta}_3x_3x_1) + \hat{c}(k_1y_1 + k_2y_2) \\ &= (\hat{\theta}_1x_2 + \hat{\theta}_2x_3 + \hat{\theta}_3x_3x_1) + \hat{c}r^{-1}(p_{21}y_1 + p_{22}y_2) \end{aligned} \quad (35)$$

Based on (23), we have:

$$\begin{aligned} \hat{\theta}_1(t) &= \gamma_1 \int_0^t x_2(p_{21}y_1 + p_{22}y_2) d\tau \\ \hat{\theta}_2(t) &= \gamma_2 \int_0^t x_3(p_{21}y_1 + p_{22}y_2) d\tau \\ \hat{\theta}_3(t) &= \gamma_3 \int_0^t x_2x_3(p_{21}y_1 + p_{22}y_2) d\tau \end{aligned} \quad (36)$$

To sum up, we obtained an optimal and adaptive controller in the form (35), (36), the implementation of which only requires measurement access to the components of the system state  $x_1, x_2, x_3$ .

**Remark 1.** Note that the approximator of the function  $f$  is represented by basis functions  $\varphi_i$  that depend on  $x_1, x_2, x_3$  (instead of on  $y_1, y_2$ ), which is not a problem due to the possibility of transforming system (24) into (28) with the third equation attached to it (see zero dynamic).

### 3.3. Optimal and Adaptive Controller Synthesis—Simplified Case

Now, with reference to Section 3.2, let it be assumed that

$$\hat{\theta} = \hat{\theta}_1, \Phi = \varphi_1 = (r_{1n}x_2 + p\psi_{0n}x_3 + pL_{1n}x_3x_1) \quad (37)$$

where the system parameters are assumed to be (reasonably) arbitrary—e.g., easily available nominal parameters (here, subscript ‘ $n$ ’).

So, the final formula for control  $u_2$  is obtained (cf. (35), (21)) in the form:

$$\begin{aligned} u_2 &= \hat{\theta}_1\varphi_1 + \hat{c}k^T\chi = \hat{\theta}_1(r_{1n}x_2 + p\psi_{0n}x_3 + pL_{1n}x_3x_1) + \hat{c}(k_1y_1 + k_2y_2) \\ &= \hat{\theta}_1(r_{1n}x_2 + p\psi_{0n}x_3 + pL_{1n}x_3x_1) + \hat{c}r^{-1}(p_{21}y_1 + p_{22}y_2) \end{aligned} \quad (38)$$

and, based on (23), the parameter estimate law is:

$$\hat{\theta}_1(t) = \gamma_1 \int_0^t (r_{1n}x_2 + p\psi_{0n}x_3 + pL_{1n}x_3x_1)(p_{21}y_1 + p_{22}y_2)d\tau \quad (39)$$

It should be noted that this version of the control algorithm, in order to improve system performance, uses additional, easily accessible knowledge contained not only in the system structure, but also in the arbitrarily adopted estimates of the system parameters.

As will be seen in the simulations carried out later, this type of adaptive controller shows good performance, which together with its relative simplicity, may be of interest for wider practical application.

**Remark 2.** In this simplified controller version, the stability proof of former section should be supplemented to deal with (include) an approximation error of function  $f$ . The relevant details, in this respect, can be found [31].

In order to clarify and facilitate the operating of formulas scattered in the text, the following briefly outlines the entire procedure:

3. Having canonical matrices  $A, B$  as in (12) and selecting criterial matrices  $Q, r$ , the Riccati Equation (20) should be solved, obtaining the matrix  $P$ ;
4. Differentiating  $y$  (or  $y_1$ ), one obtains  $y_2$  (26);
5. Using the model basis function  $\Phi$  (see (34) or (37)), current estimates of parameters  $\hat{\theta}$  are obtained via formulas (36) or (39);
6. By the formula (35) or (38), the dynamical controller  $u_2$  is obtained,
7. Set the design parameter  $\hat{c}$  to obtain a satisfactory system performance.

### 3.4. Resetting Reactive Power by the Second Control Input Synthesis—System Energetic Optimization

Now, having the second control parameter at our disposal ( $u_1$ ), one can modify the control process in terms of affecting the value of the object’s steady-state signals.

In this context, it seems reasonable to perform an energetic optimization of the system operation, i.e., to guarantee that the system reactive power equals zero:

$$Q = 1.5(U_qI_d - U_dI_q) = 1.5(u_2x_1 - u_1x_2) = 0 \quad (40)$$

To this end, one can observe that a simple transformation of (40) yields

$$u_1 = \frac{x_1}{x_2} u_2 \text{ or } U_d = \frac{I_d}{I_q} U_q \quad (41)$$

This means that having access to the system state and control  $u_2$ , generated via dynamic controller (35) or (38) (see previous section), a respective control  $u_1$  can be easily found that guarantees the condition (40), i.e., the zeroing of reactive power consumption.

### 3.5. Analysis the System Zero Dynamics

The partial transformation of the coordinates from  $x$  to  $y$  is defined by the equations in (29). After this transformation, a new system (28) of the second order, representing the external dynamics, is obtained. As the original system (24), (25) is of the third order, the missing part of the dynamics should be completed with the internal (zero) dynamics (of the first order). The proof of stability of the internal dynamics plays a key role in the successful application of the I/O linearization method, as it guarantees the stability of the whole (original) system (24).

To analyze the system zero dynamics, it is enough to examine the original system (24), (25), assuming that its output is precisely equal to zero. This leads to the system's restricted motion [32] being confined to the set:

$$Z^* = \left\{ x : h(x) = L_f h(x) = 0 \right\} = \left\{ x : x_3 - x_3^* = 0 ; \frac{1.5p\psi_0}{J} x_2 - \frac{T_L}{J} = 0 \right\} = \left\{ x : x_3 = \omega_m ; x_2 = \frac{T_L}{1.5p\psi_0} \right\} \quad (42)$$

where

$$y = h(x) = x_3 - x_3^*$$

and  $L_f h(x) = \frac{\partial h}{\partial x} f$  denotes the Lie derivative.

The motion of the original system (24), (25) on  $Z^*$ , with the input [32]

$$u_2^* = \frac{-f(x)}{g(x)} \Big|_{x \in Z^*} = -pL_1 x_3 x_1 - r_1 x_2 - p\psi_0 x_3$$

represents the system zero dynamics:

$$\frac{dx_1}{dt} = -\frac{r_1}{L_1} x_1 + p x_3 x_2 + \frac{1}{L_1} u_1 \quad (43)$$

As the term  $p x_3 x_2 = \text{const}$  (see (42)) and as  $u_1$  is bounded (and constant in a steady state), this dynamics takes the form of a stable linear system:

$$\frac{dx_1}{dt} = -\frac{r_1}{L_1} x_1 + \text{const} \quad (44)$$

In this way, it is proven that the control (35) or (38) found above stabilizes the entire nonlinear system (24).

## 4. Results

The system of adaptive PMSM control of the ship's electric propulsion system with energy optimization possibility in an INV-PMSM circuit ( $Q = 0$ ), as presented in this article, is shown in Figure 2.

The simulation studies presented below, which are used to verify the performance of the designed control algorithm, were based on the PMSM nonlinear dynamic model (1), (2), (3) as being representative of a real machine.

The model parameters were adopted as shown in Table 1:

Table 1. Parameters of the tested permanent magnet synchronous motor (PMSM).

DC Circuit Voltage $U_{dc}$ (V)	Stator Winding Resistance, $r_1$ (m $\Omega$ )	Inductance of the Stator Windings, $L_1$ (mH)	Mechanical Speed, $\omega_m$ (1/s)	Number of Pole Pairs, $p$	Flux Linkage $\Psi_0$ (Wb)	Inertia $J$ (kgm <sup>2</sup> )	Nominal Electromagnetic Torque $T_{eN}$ (Nm)
560	0.05	0.635	314.15	4	0.192	0.011	126

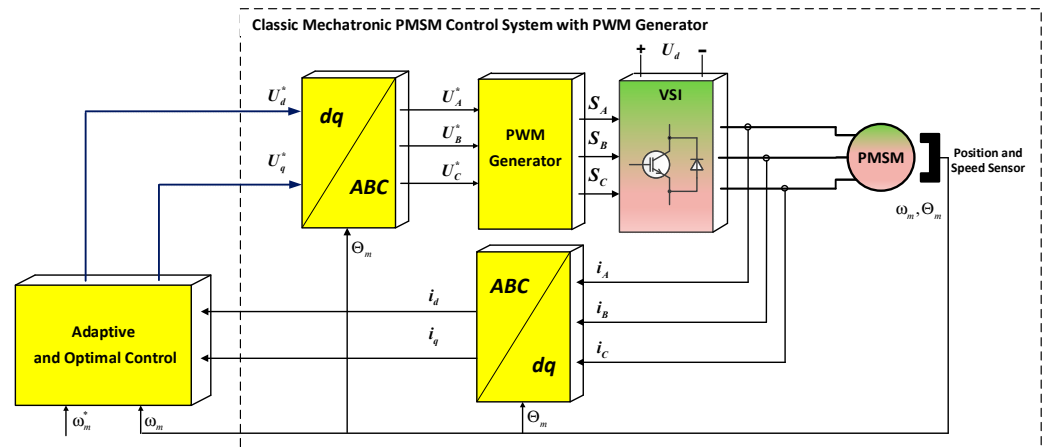


Figure 2. Adaptive control system of PMSM with energy optimization possibility in INV–PMSM circuit ( $Q = 0$ ) implemented in Matlab–Simulink program.

During the test, variations in machine speed  $\omega_m$ , load torque  $T_L$ , stator currents  $I_d, I_q$ , active  $P$  and reactive power  $Q$  were recorded, as well as the process of tuning parameter estimates, all vs. time. The results of the test, presented in Figures 3–5, are as follows: Figure 3 depicts, respectively, the actual machine speed  $\omega_m$  in relation to the reference speed  $\omega_m^*$ , load torque  $T_L$  related to the electromagnetic moment  $T_e$ , stator currents  $I_d$  and  $I_q$ , active  $P$  and reactive power  $Q$ .

In the figures below, (a) refers to the basic case, while (b) refers to the simplified case.

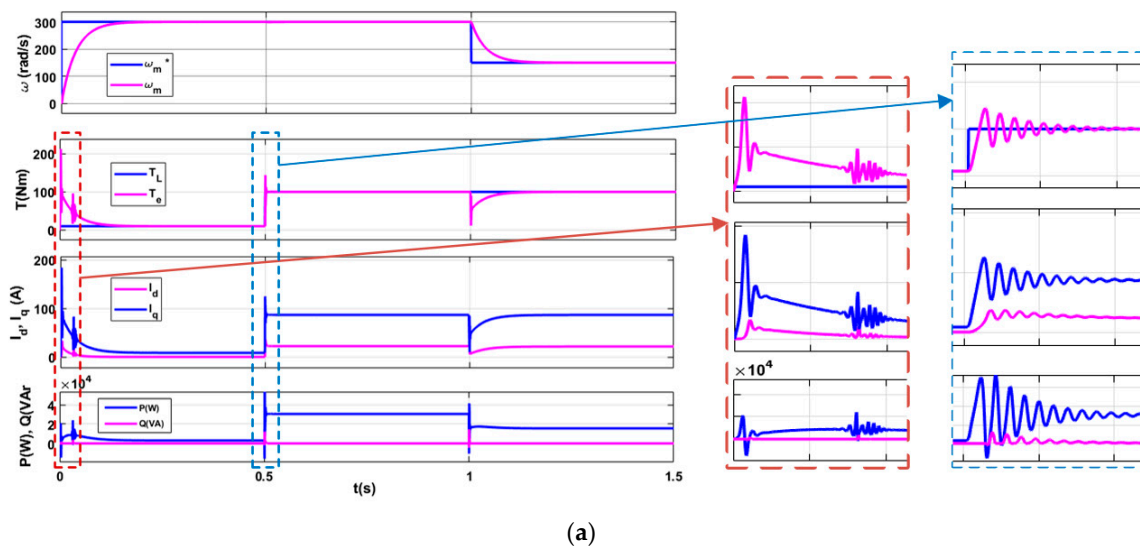


Figure 3. Cont.

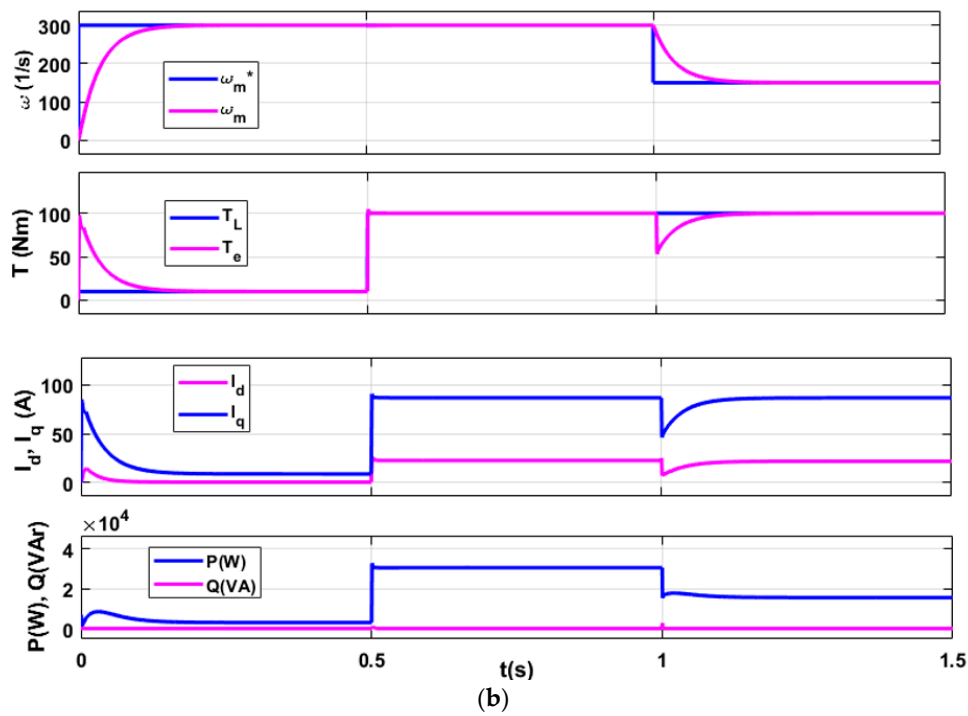


Figure 3. (a) Waveforms of the speeds, torques, currents and powers vs. time; basic case. (b) Waveforms of the speeds, torques, currents and powers vs. time; simplified case.

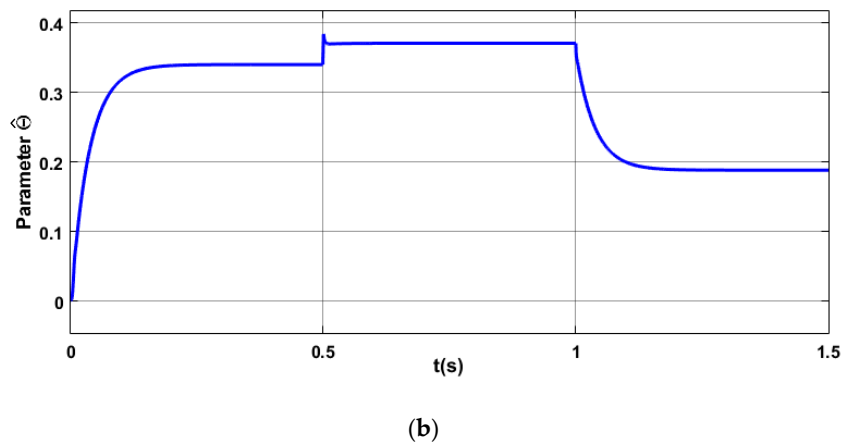
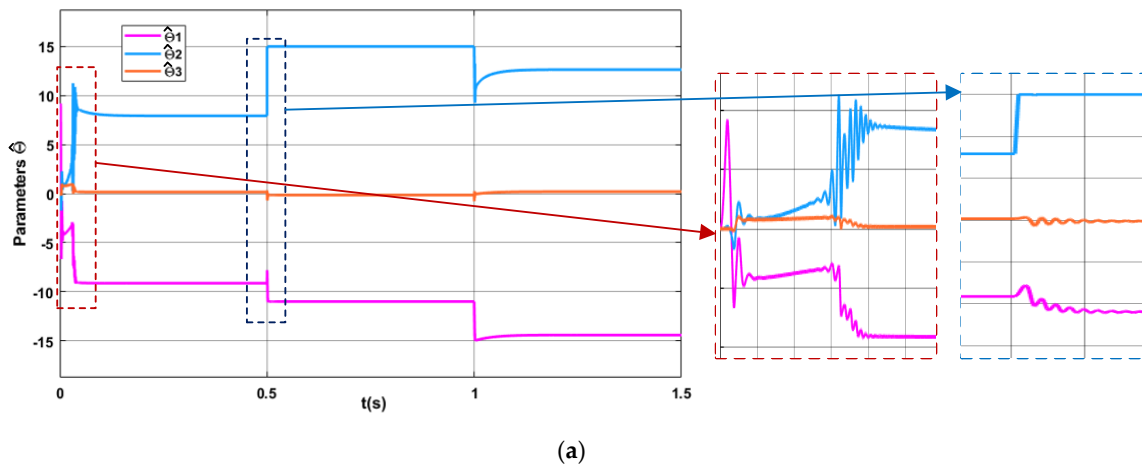
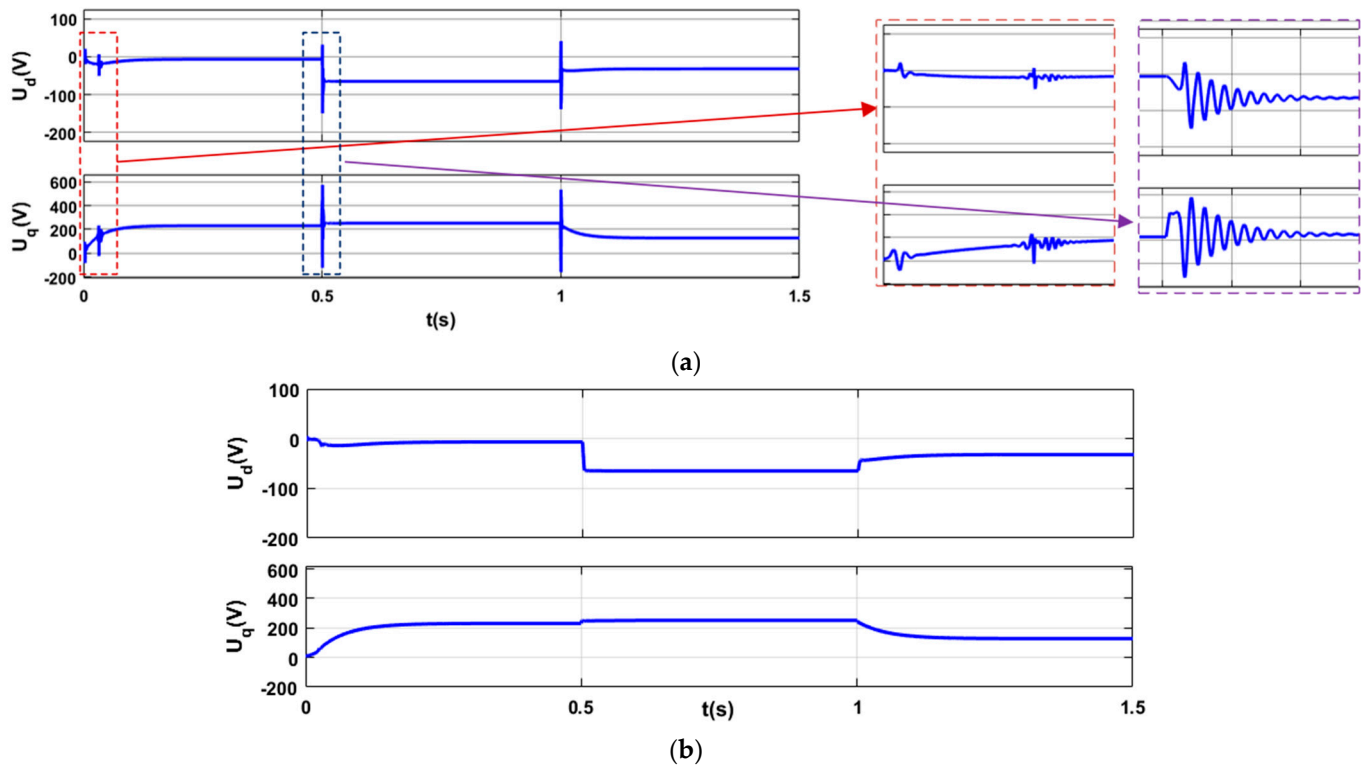


Figure 4. (a) Variations in system parameters  $\hat{\theta}(t)$  vs. time; basic case. (b) Variations in system parameters  $\hat{\theta}(t)$  vs. time; simplified case.



**Figure 5.** (a) Control signals in the form of voltages  $U_d$  and  $U_q$  vs. time; basic case. (b) Control signals in the form of voltages  $U_d$  and  $U_q$  vs. time; simplified case.

As can be observed in Figure 3, the set speed of 300 rad/s was changed to 150 rad/s after 1 s, while the load torque was changed from 10 Nm to 100 Nm after 0.5 s.

It can be seen that after a step change in operating conditions, i.e., speed or/and load, there is an immediate fine-tuning of the controller parameters (Figure 4) ensuring stable system operation. The dynamics of the transition processes for the mechanical quantities is correct with perfect resistance to load disturbances. However, the transients of electrical signals, as, e.g., voltages, (Figure 5a)), exhibit at the switching moments peaks, which are decaying oscillations caused by the abrupt nature of the changes in the set value of  $\omega_m$  or disturbances ( $T_L$ ) and subsequent rapid changes in the tunable parameters, under the new operating conditions. Observe that in the simplified case, the abrupt peaks are relatively negligible. This is due to the fact that we have only one parameter to tune, as well as the fact that the difference between the standard zero initial conditions, during its tuning, and its final value is much smaller. The reactive power is maintained at zero at all times, as postulated.

During the numerical experiment, it was assumed that  $Q = 10^7[10\ 0; 0\ 0.1]$ ,  $r = 1$ , designed parameter  $c_d = 10\hat{c}$ , and tuning parameter  $\gamma_i = \gamma = 10^{-7}$ . However, in the simplified case, in addition, it was assumed that  $r_{1n} = 0.1r_1$ ,  $\psi_{0n} = 10\psi_0$ , and  $L_{1n} = 100L_1$ . As can be seen, despite the quite arbitrarily adopted parameters in the simplified case, the system works better than in the basic case. This is due to the fact that in the (simplified) case, some very preliminary, but still relevant knowledge, about the object parameters is obtained, whereas in the general (basic) case, there is no knowledge at all.

The basic case (a) of adaptive control assumes no knowledge of the PMSM parameters  $r_1, \psi_0, L_1$ . During engine start-up, parameters  $\hat{\theta}_1, \hat{\theta}_2, \hat{\theta}_3$ , with an initial value of 0, must rapidly adjust to the equilibrium points (Figure 4a). This causes a transient in the voltage values  $U_d^*, U_q^*$  provided by the controller (Figure 5a), the symptom of which is torque jitter (Figure 3a). The case of simplified adaptive control (b) assumes approximate knowledge (order of magnitude) of the PMSM parameter values on which the controller is based. This

fact makes it easier to tune the parameter  $\hat{\theta}$  (here, a single one) so that oscillations do not occur during the transition period (Figures 3b, 4b and 5b).

In the case of classical PMSM control, according to the FOC method, as already mentioned in the introduction, the INV-PMSM electrical circuit analysis is only valid for the steady state.

Transients (e.g., speed changes) are not adequately controlled, resulting in significant oscillations, e.g., in torque [11,12]. Attempts to optimize the settings of the PID controller used in the FOC method do not yield good results in this respect.

## 5. Discussion and Conclusions

The main idea of the paper is to design a controller for PMSM machine. Its general concept is based on some known, canonical system dynamics with a function to adapt it to the real dynamics by adjusting the unknown parameters.

The applied methods of baseline controller design and its parameters tuning are based on optimal and adaptive techniques from the field of control theory, i.e., LQR and direct adaptive control, combined with the output feedback linearization.

More specifically, the system with canonical matrices  $A$  and  $B$ , which represent some basic system dynamics, is tuned to follow the real system via the adaptation of parameters.

Simulation tests have shown that the control system designed via the control techniques applied here ensures a fast transient response and good load disturbance resistance response, and unlike a standard PID controller, does not require the troublesome adjustment of its settings. Moreover, it reduces the reactive power of the system to zero.

The authors proposed an original adaptive PMSM control that does not require accurate machine rating data, as is the case with classic PMSM control according to the FOC method using PID controllers. The control algorithm developed by the authors also ensures energy optimization by reducing reactive power in the INV-PMSM circuit. The authors found no descriptions in the literature of adaptive PMSM control systems based on input–output linearization, LQR and reactive power reduction techniques in the INV-PMSM circuit being implemented at the same time.

The proposed adaptive system is characterized not only by robustness to the effects of load disturbances, but mainly by the fact that it does not need to be tuned, which is a major problem for standard PID-type controllers. The controller synthesis in the simplified case appears to be particularly attractive for practical implementation, because using standard, uncertain knowledge available ‘at hand’, we can achieve very good, cost-free control performance.

Currently, the authors are in the process of completing the construction of a laboratory station with a PMSM drive based on a new technology, i.e., Speedgoat hardware in the Rapid Control Prototyping mode [33]. It should be noted here that the simulation model developed in Matlab-Simulink used in the article can be easily used during laboratory experiments. Speedgoat’s powerful prototyping hardware with a flexible and easy-to-use I/O is 100% compatible with Matlab-Simulink. In their next article, the authors intend to present the results of an experimental research study.

**Author Contributions:** Conceptualization, Z.Z., D.T. and A.N.; methodology, Z.Z., D.T. and A.N.; software, Z.Z.; validation, Z.Z., D.T. and A.N.; formal analysis, Z.Z.; investigation, Z.Z.; writing—original draft preparation, Z.Z. and D.T.; writing—review and editing Z.Z., D.T. and A.N.; visualization, Z.Z. and D.T. All authors have read and agreed to the published version of the manuscript.

**Funding:** This research received no external funding.

**Data Availability Statement:** The data presented in this study are available from the corresponding authors upon reasonable request.

**Conflicts of Interest:** The authors declare no conflicts of interest.

## References

1. Reusser, C.A.; Young, H.A.; Perez Osses, J.R.; Perez, M.A.; Simmonds, O.J. Power Electronics and Drives: Applications to Modern Ship Propulsion Systems. *IEEE Ind. Electron. Mag.* **2020**, *14*, 106–122. [CrossRef]
2. Polakis, M.; Zachariadis, P.; Kat, J.O. The Energy Efficiency Design Index (EEDI). In *Sustainable Shipping*; Springer: New York, NY, USA, 2019; pp. 93–135. [CrossRef]
3. Implementing Energy Efficiency Design Index (EEDI). Indian Register of Shipping (IRClass). Available online: [www.irclass.org/media/2368/energy-efficiency-design-index.pdf](http://www.irclass.org/media/2368/energy-efficiency-design-index.pdf) (accessed on 10 January 2024).
4. Zwierzewicz, Z.; Tarnapowicz, D.; German-Galkin, S.; Jaskiewicz, M. Optimal Control of the Diesel–Electric Propulsion in a Ship with PMSM. *Energies* **2022**, *15*, 9390. [CrossRef]
5. Dambrauskas, K.; Vanagas, J.; Zimnickas, T.; Kalvaitis, A.; Ažubalis, M. A Method for Efficiency Determination of Permanent Magnet Synchronous Motor. *Energies* **2020**, *13*, 1004. [CrossRef]
6. Deusinger, B.; Lehr, M.; Binder, A. Determination of efficiency of permanent magnet synchronous machines from summation of losses. In Proceedings of the 2014 International Symposium on Power Electronics, Electrical Drives, Automation and Motion, Ischia, Italy, 18–20 June 2014; pp. 619–624.
7. Puranen, J. Permanent Magnet Machine vs. Induction Machine for In-Line Shaft Generator System. Theswitch, Version 1, 9/2021. Available online: [https://theswitch.com/wp-content/uploads/2022/02/Marine\\_Talking\\_point\\_EN\\_PMM\\_IM\\_SG\\_comparison\\_20210929.pdf](https://theswitch.com/wp-content/uploads/2022/02/Marine_Talking_point_EN_PMM_IM_SG_comparison_20210929.pdf) (accessed on 12 March 2023).
8. Kirtley, J.K.; Banerjee, A.; Englebretson, S. Motors for Ship Propulsion. *Proc. IEEE* **2015**, *103*, 2320–2332. [CrossRef]
9. Jamieson, P. *Innovation in Wind Turbine Design*; John Wiley & Sons, Ltd.: Hoboken, NJ, USA, 2011; ISBN 9780470699812.
10. Zawirski, K.; Deskur, J.; Kaczmarek, T. *Electric Drive Automation*; Poznan University of Technology Publishing House: Poznan, Poland, 2012; ISBN 978-83-7775-160-2.
11. Kaczmarek, T.; Zawirski, K. *Drive Systems with Synchronous Motor*; Poznan University of Technology Publishing House: Poznań, Poland, 2000; ISBN 978-83-7348-401-6.
12. Kazmierkowski, M.P.; Irwin, J.D.; Krishnan, R.; Blaabjerg, F. *Control in Power Electronics. Selected Problems*, 1st ed.; Elsevier: Amsterdam, The Netherlands; Academic Press: Cambridge, MA, USA, 2002; ISBN 9780124027725.
13. Kazmierkowski, M.P.; Tunia, H. *Automatic Control of Converter-Fed Drives*, 1st ed.; Elsevier: Amsterdam, The Netherlands, 1994; Volume 46, ISBN 9780444986603.
14. Alfahaid, A.A.; Strangas, E.G.; Khalil, H.K. Speed control of Permanent Magnet Synchronous Motor using extended high-gain observer. In Proceedings of the 2016 American Control Conference (ACC), Boston, MA, USA, 6–8 July 2016; pp. 2205–2210. [CrossRef]
15. Tarnapowicz, D.; Zaleski, T.; Matuszak, Z.; Jaskiewicz, M. Energy Optimization of Marine Drive Systems with Permanent Magnet Synchronous Motors. *Energies* **2024**, *17*, 31. [CrossRef]
16. Vimal, M.; Sojan, V. Vector controlled PMSM drive with power factor correction using zeta converter. In Proceedings of the 2017 International Conference on Energy, Communication, Data Analytics and Soft Computing (ICECDS), Chennai, India, 1–2 August 2017; pp. 289–295.
17. Ho, T.-Y.; Chen, M.-S.; Chen, L.-Y.; Yang, L.-H. The design of a PMSM motor drive with active power factor correction. In Proceedings of the 2nd International Conference on Artificial Intelligence, Management Science and Electronic Commerce (AIMSEC), Dengfeng, China, 8–10 August 2011; pp. 4447–4450.
18. Yin, Y.; Liu, L.; Vazquez, S.; Xu, R.; Dong, Z.; Liu, J.; Leon, J.I.; Wu, L.; Franquelo, L.G. Disturbance and Uncertainty Attenuation for Speed Regulation of PMSM Servo System Using Adaptive Optimal Control Strategy. *IEEE Trans. Transp. Electrification* **2023**, *9*, 3410–3420. [CrossRef]
19. Tan, L.N.; Pham, T.C. Optimal Tracking Control for PMSM With Partially Unknown Dynamics, Saturation Voltages, Torque, and Voltage Disturbances. *IEEE Trans. Ind. Electron.* **2022**, *69*, 3481–3491. [CrossRef]
20. Rathod, G.; Thosar, A.G.; Dhote, V.P.; Zalke, R. PM Synchronous Motor Drive for Electric Vehicles by Using an Adaptive Controller. In Proceedings of the 2018 International Conference on Emerging Trends and Innovations In Engineering and Technological Research (ICETIETR), Ernakulam, India, 11–13 July 2018; pp. 1–5. [CrossRef]
21. German-Galkin, S.; Tarnapowicz, D. Energy Optimization of the ‘Shore to Ship’ System—A Universal Power System for Ships at Berth in a Port. *Sensors* **2020**, *20*, 3815. [CrossRef] [PubMed]
22. Slotine, J.E.; Li, W. *Applied Nonlinear Control*; Prentice Hall: Englewood Cliffs, NJ, USA, 1991; ISBN 0-13-040890-5.
23. Zwierzewicz, Z. Design of ship course-keeping system via robust adaptive approach. In Proceedings of the 2017 22nd International Conference on Methods and Models in Automation and Robotics (MMAR), Miedzyzdroje, Poland, 28–31 August 2017; pp. 101–106. [CrossRef]
24. Zwierzewicz, Z. Nonlinear adaptive tracking-control synthesis for functionally uncertain systems. *Int. J. Adapt. Control Signal Process.* **2010**, *24*, 96–105. [CrossRef]
25. Tau, J.-H.; Tzou, Y.-Y. PFC control of electrolytic capacitor-less PMSM drives for home appliances. In Proceedings of the IEEE 26th International Symposium on Industrial Electronics (ISIE), Edinburgh, UK, 19–21 June 2017; pp. 335–341.
26. Gokulapriya, R.; Pradeep, J. Shunt based active power factor correction circuit for direct torque controlled PMSM drive. In Proceedings of the Third International Conference on Science Technology Engineering & Management (ICONSTEM), Chennai, India, 23–24 March 2017; pp. 517–521.

27. Cimini, G.; Ippoliti, G.; Orlando, G.; Pirro, M. PMSM control with power factor correction: Rapid prototyping scenario. In Proceedings of the 4th International Conference on Power Engineering, Energy and Electrical Drives, Istanbul, Turkey, 13–17 May 2013; pp. 688–693.
28. Moussa, M.F.; Helal, A.; Gaber, Y.; Youssef, H.A. Unity Power Factor control of permanent magnet motor drive system. In Proceedings of the 12th International Middle-East Power System Conference, Aswan, Egypt, 12–15 March 2008; pp. 360–367.
29. Tengfei, L.; Cong, W. Learning from neural control of general Brunovsky systems. In Proceedings of the 2006 IEEE Conference on Computer Aided Control System Design, 2006 IEEE International Conference on Control Applications, 2006 IEEE International Symposium on Intelligent Control, Munich, Germany; 2006; pp. 2366–2371. [[CrossRef](#)]
30. De Larminat, P. *Analysis and Control of Linear Systems*; Wiley-ISTE: Hoboken, NJ, USA, 2007; ISBN 9781905209354.
31. Zwierzewicz, Z. Robust and Adaptive Path-Following Control of an Underactuated Ship. *IEEE Access* **2020**, *8*, 120198–120207. [[CrossRef](#)]
32. Khalil, H.K. *Nonlinear Systems*, 3rd ed.; Prentice Hall: Upper Saddle River, NJ, USA, 2002; pp. 509–521, ISBN 978-0130673893.
33. Speedgoat. Rapid Control Prototyping. Available online: <https://www.speedgoat.com/solutions/testing-workflows/rapid-control-prototyping> (accessed on 12 December 2023).

**Disclaimer/Publisher’s Note:** The statements, opinions and data contained in all publications are solely those of the individual author(s) and contributor(s) and not of MDPI and/or the editor(s). MDPI and/or the editor(s) disclaim responsibility for any injury to people or property resulting from any ideas, methods, instructions or products referred to in the content.